Dual-scale artificial lotus leaf fabricated by fully nonlithographic simple approach based on sandblasting and anodic aluminum oxidation techniques

Seung-Jun Kim [a,1], Tae-Hyun Kim [a,1], Jeong-Ho Kong [a], Yongsung Kim [b], Chae-Ryong Cho [c], Soo-Hyung Kim [a], Deug-Woo Lee [a], Jong-Kweon Park [d], Dongyun Lee [e,*], Jong-Man Kim [a,*]

[a] Department of Nanomechatronics Engineering, Pusan National University, Busan 609-735, Republic of Korea
[b] Samsung Advanced Institute of Technology, Samsung Electronics, Yongin 446-712, Republic of Korea
[c] Department of Applied Nanoscience, Pusan National University, Busan 609-735, Republic of Korea
[d] Korea Institute of Machinery and Materials, Daejeon 305-343, Republic of Korea
[e] Department of Nanofusion Engineering, Pusan National University, Busan 609-735, Republic of Korea

ABSTRACT

This paper reports a micro/nano dual-scaled artificial lotus leaf that is formed on a silicon substrate by simple and inexpensive fully nonlithographic approach, combining a sandblasting technique and an anodic aluminum oxidation (AAO) process. The proposed dual-scaled surface was demonstrated by covering the sandblasted micro-roughened substrate entirely with nano-scale protuberances, and its surface wettability was characterized by measuring the static contact angle (SCA) and contact angle hysteresis (CAH). The measurements confirmed that the proposed dual-scaled surface can sufficiently ensure superhydrophobicity in the Cassie wetting regime with a high SCA of $159.4 \pm 0.5°$ and a low CAH of $3.9 \pm 0.7°$, and the surface wetting properties can be improved greatly compared to those of flat, sandblasted micro-roughened and nano-scale protuberance-arrayed surfaces. Through a dropping test, it was observed that the fabricated dual-scaled surface can ensure its superior water-repellency with various levels of the impact velocity. Finally, a self-cleaning ability of the proposed dual-roughened surface was verified experimentally by observing the dynamic rolling-off behavior of the water droplet on the surface covered with contaminants.

© 2012 Elsevier B.V. All rights reserved.

1. Introduction

Recent advances in micro- and nano-fabrication technologies have made it possible to realize a range of functional three-dimensional structures precisely in micro/nano-sized regimes, and their application fields have been expanded constantly from stand-alone structures to micro/nano-scale devices. Nowadays, the demonstration of a superhydrophobic surface that is based on micro/nano double-sized structures to mimic a lotus leaf in nature is one of the most attractive application targets because it has been verified both experimentally and theoretically that such surfaces modified geometrically with multi-scale roughness show superior wetting properties compared to only chemically-treated and mono-scale roughened ones [1–3]. Therefore, a wide range of fabrication approaches have been proposed to realize a

hierarchically textured functional surface ensuring superhydrophobicity [4–12]. On the other hand, in most methods reported in the literature, the lithographic processes were generally contained on their fabrication procedures to define the surface geometry with the micro- and nano-sizes. Although these lithography-based fabrication approaches are desirable for enhancing and controlling the wetting properties of such surfaces by realizing shape-controllable structures with geometrical regularity, the fabrication complexity is unavoidable due to their multi processing steps. Therefore, many attempts have been made to create a hierarchically textured surface based on fully non-lithographic processes, such as plasma etching, electrochemical etching, heat treatment, colloidal self assembly, laser ablation, molding/replication, etc. [13–19]. Although some of the non-lithographic approaches can fairly alleviate the complexity in fabrication, specific process conditions must be imposed to create multi-scale roughness on the surface. In addition, in some cases, the nonlithographic method can be applied restrictively only on specific substrate materials because the micro and/or nano structures can be generated through the specified reactions. Therefore,

* Corresponding authors.
  E-mail addresses: dlee@pusan.ac.kr (D. Lee), jongkim@pusan.ac.kr (J.-M. Kim).
[1] Both authors contributed equally to this work as co-first authors.

these limitations make it difficult to achieve reproducibility and applicability of the textured surface. The sandblasting technique is a common way of abrading a surface by jetting the abrasives to the targeted surface. This can be also used to realize textured surfaces to improve the surface wettability efficiently by increasing the surface roughness on the micro-scale. In particular, the sandblasting process can provide the simplicity in fabrication without any specific and complex conditions, and also be applied to a large area surface. Owing to these advantageous aspects of the sandblasting method, some research groups have chosen it to create micro-roughened surfaces [20–22]. Although they can create dual-roughened superhydrophobic surfaces by hierarchically constructing nano-scale roughness on the sandblasted surface with fully nonlithographic strategies, some problems are still remained. The tedious process, such as a replication with specified conditions, is still needed, or the usable substrate is limited specifically to the surfaces that can react chemically in subsequent processes, such as surface oxidation and electrolytic etching.

This paper proposes a simple and highly applicable method to mimic the lotus leaf efficiently by creating micro/nano dual-scale roughness using the nonlithographic sandblasting technique and subsequent wet oxidation of thin-film aluminum. The advantages of the proposed fabrication method can be summarized as follows. Simple non-lithographic processes without the specific conditions/equipments and subsequent low-energy surface coating make it possible to create a dual-scale superhydrophobic surface more easily and reproductively. Moreover, it is less restrictive to the selection of the substrate materials because nano-scale protuberances are formed subsequently in any type of substrate after sandblasting, resulting in higher applicability. In addition, the proposed method is highly practicable because it is also suitable to a large area process due to stabilized sandblasting and anodic aluminum oxidation (AAO) technologies. The superior superhydrophobicity of the proposed dual-scaled surface is verified experimentally through static wettability analysis, dropping and practical self-cleaning tests.

2. Experiment details

2.1. Fabrication of micro/nano dual-scaled surfaces

Fig. 1 shows a fabrication procedure of the micro/nano dual-scaled surface proposed in this paper. Initially, micro-roughness was formed on a silicon substrate using a sandblasting technique. For this, a 4-in. silicon wafer was first abraded by jetting the Al_2O_3 micro-particles under a water pressure of 0.2 MPa using a commercially available sandblasting system (SATech) with two individual jetting nozzles. The sandblasted silicon wafer was then cleaned with a 4:1 aqueous mixture of H_2SO_4 and H_2O_2. A 2-μm-thick aluminum layer was deposited on the sandblasted silicon substrate by RF magnetron sputtering. Subsequently, anodization and pore-widening processes were performed sequentially on the sputter-deposited aluminum layer, to cover the micro-roughened surface with a nano-scale roughness hierarchically by forming nano-scale alumina protuberances entirely. In this case, the anodization process was carried out in a 0.3 M oxalic electrolytic solution with an applied voltage and a temperature of 100 V and 0 °C, respectively, for 4 min. In particular, the anodization process was repeated twice under the same conditions to increase the pore regularity of the porous alumina membrane (PAM). After the anodization processes, the nano-protuberance arrays were formed on the micro-roughened surface entirely by etching the sidewalls between the adjacent pores on the PAM using 5 wt% phosphoric acid with a constant temperature of 30 °C for 100 min. Finally,
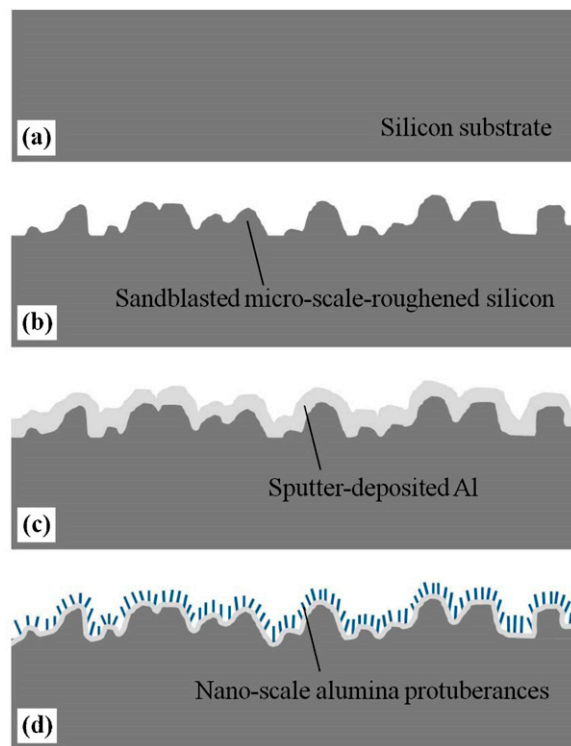

Fig. 1. Fabrication procedure of the proposed micro/nano dual-scaled superhydrophobic surface. (a) Flat silicon substrate, (b) sandblasting of the silicon substrate, (c) aluminum deposition, (d) aluminum anodization and subsequent pore-widening (formation of nano-scale protuberance array).

a thin-film fluorocarbon (FC) layer was deposited on the fabricated dual-scaled surface by a continuous C_4F_8 glow discharge to hydrophobize the surface. The hydrophobic surface coating was performed under a gas flow rate and applied power of 100 sccm and 800 W, respectively, for 30 s. The dual-scaled superhydrophobic surface was prepared using the fully nonlithographic simple processes described above. On the other hand, the proposed hierarchical approach can also be applied to any substrate material, which can be roughened in micro-scale by sandblasting, such as transparent glass and quartz, various metallic sheets as well as silicon substrates. A silicon wafer was used in this study as the substrate for convenience. In this experiment, four kinds of samples with different surface geometries (flat, sandblasted micro-roughened, nano-scale protuberance-arrayed, and micro/nano dual-scaled surfaces) were fabricated for comparison. The surface morphology of the fabricated surfaces was characterized by a field emission scanning electron microscopy (FE-SEM; HITACHI, S4700). In addition, to investigate the textured surfaces more precisely, the surface morphology was measured by an atomic force microscopy (AFM; Park Systems, XE-100) in non-contact mode under a scan rate of 1 Hz.

2.2. Evaluation of surface wettability

The surface wettability of the fabricated surfaces was evaluated by measuring the static contact angle (SCA) and contact angle hysteresis (CAH) using a contact angle goniometer (Dataphysics, OCA 10) equipped with a CCD camera. After a low-energy hydrophobic coating with a thin-film FC, the static wetting properties of each surface were characterized by measuring the SCAs using a sessile drop method. The measurements were performed on more than five different regions for the flat, micro-, nano- and micro/nano dual-roughened surfaces with a deionized (DI)
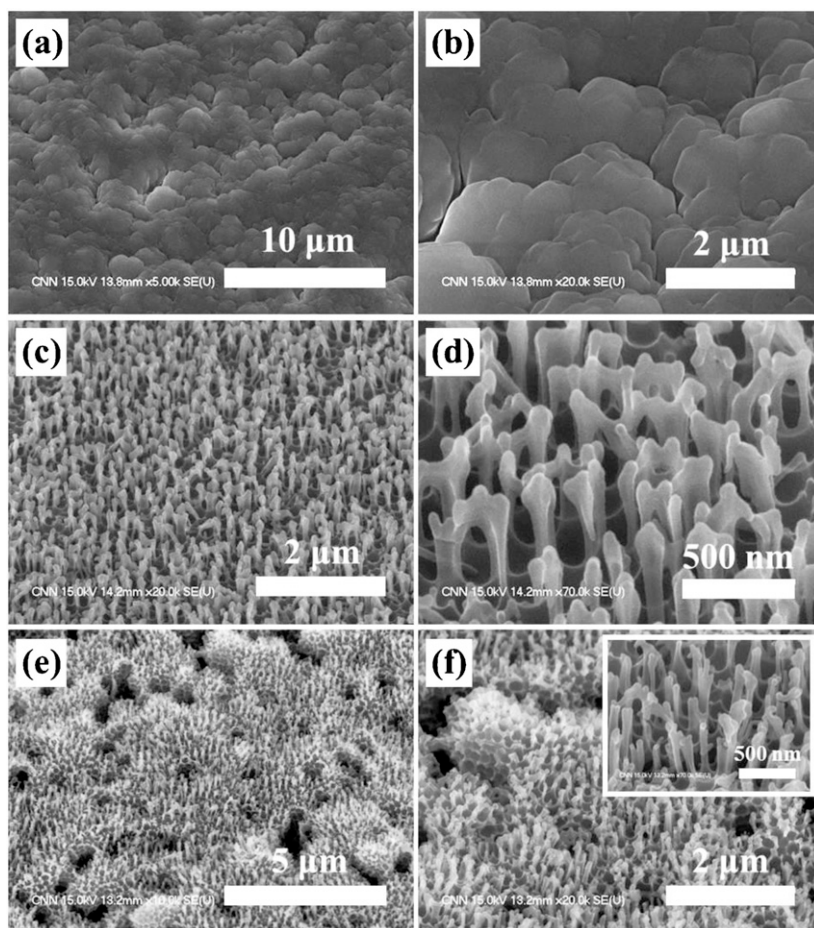
Fig. 2. SEM images of the fabricated surfaces with different geometries after the FC coating. (a) and (b) Sandblasted micro-roughened surfaces, (c) and (d) nano-scale pillar-like protuberance-arrayed surfaces, and (e) and (f) micro/nano dual-scaled surfaces (inset: magnified view of the nano-scale protuberances on the micro-roughened surface).

wafer droplet of 10 μL. The CAHs for each surface were also measured and compared to observe the effect of the proposed dual-scaled surface on the dynamic surface wettability. The CAHs were obtained experimentally by calculating the differences between the advancing and receding CAs, which were measured as the droplet volume was increased and decreased continuously, respectively, on more than five different regions of the surfaces.
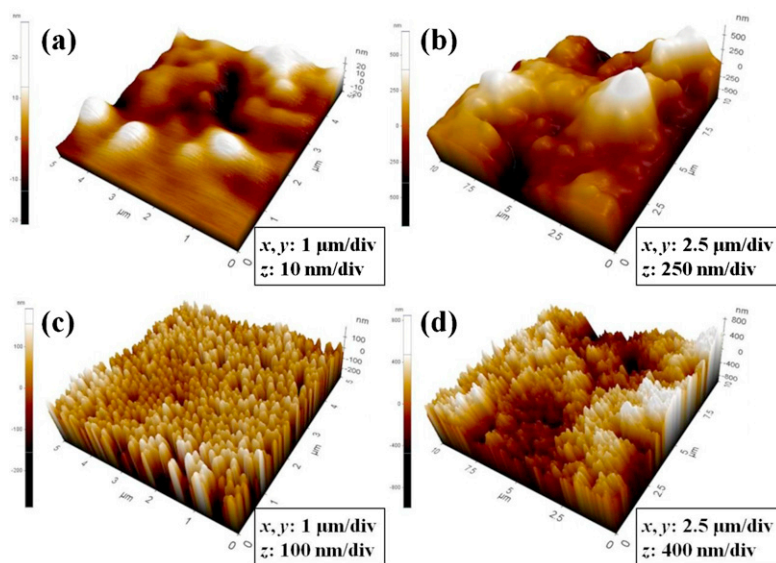

Fig. 3. AFM images of the fabricated surfaces with different geometries after the FC coating. (a) Flat silicon surface, (b) sandblasted micro-roughened surface, (c) nano-scale protuberance-arrayed surface, and (d) micro/nano dual-scaled surface.
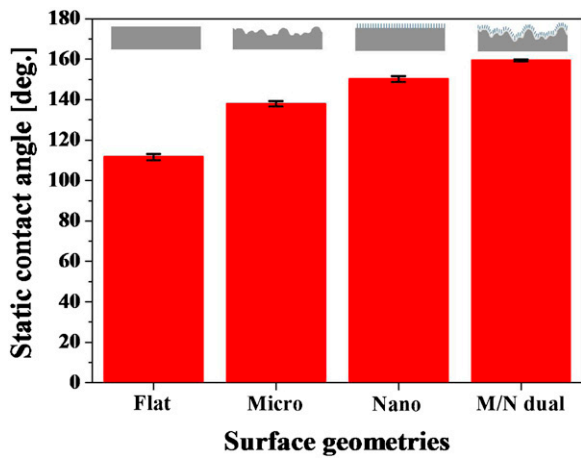
Fig. 4. Static contact angles measured on the surfaces with four different geometries.

Fig. 6. Contact angle hysteresis examined on the surfaces with four different geometries.

2.3. Dropping test

The water-repellent property of the fabricated dual-scaled surface was demonstrated by observing the impact dynamics of the water droplet on the surface. Firstly, a 10 μL water droplet was dispensed by a micropippet at initial height of ~20 mm above the surface and the falling droplet was recoded in real-time using a digital high-speed video camera (Kodak, SR-Ultra-C) with a maximal frame rate of 10,000 frames/s.

2.4. Practical self-cleaning test

A self-cleaning ability of the proposed micro/nano dual-scaled surface was demonstrated experimentally by observing dynamic behavior of the water droplets rolling off a surface contaminated with dust particles. Firstly, the silica powders (silicon (IV) oxide 99.8% metal basis, Alfa Aesar) with the average diameter of ~7 μm, which act as the dust particles in this demonstration, were
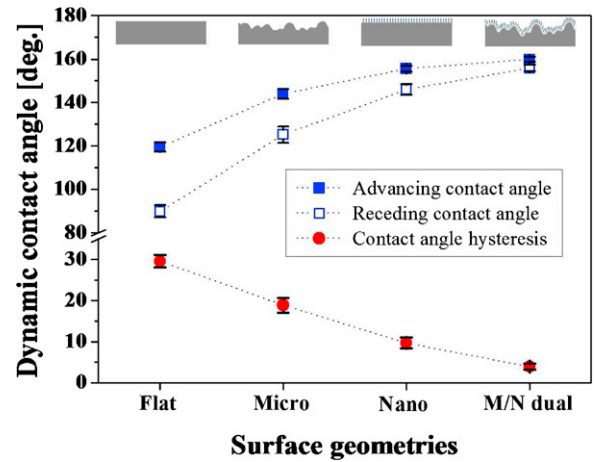
sprinkled manually on the fabricated dual-roughened surface. A DI water droplet was then dispensed on the surface, which is tilted approximately <10°, by a micropipette and a video clip of the water droplet rolling off the surface was recorded in real-time.

3. Results and discussion

3.1. Fabrication results

Fig. 2 shows SEM images of the fabricated surfaces with different geometries after the FC coating. As shown in Fig. 2(a) and (b), the micro-roughness was defined well on the silicon substrate by the sandblasting process. In addition, Fig. 2(c) and (d) clearly shows that the nano-scale pillar-like protuberances were formed regularly across the substrate by the time-controlled wet etching of the PAM in the pore-widening process. Moreover, the micro/nano dual-scaled surface was fabricated successfully by covering wholly the sandblasted micro-roughened surface with nano-scale pillar-like
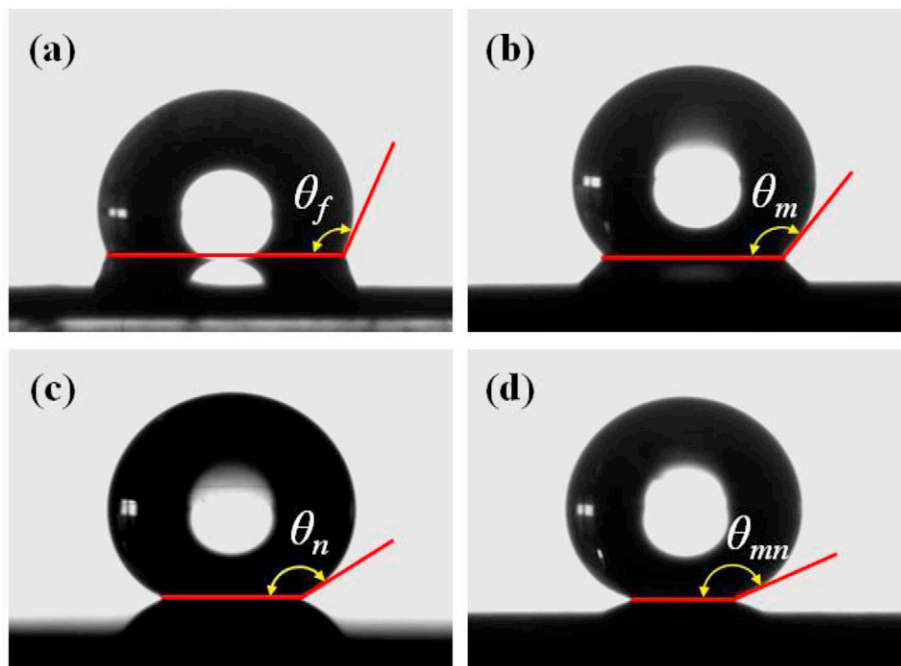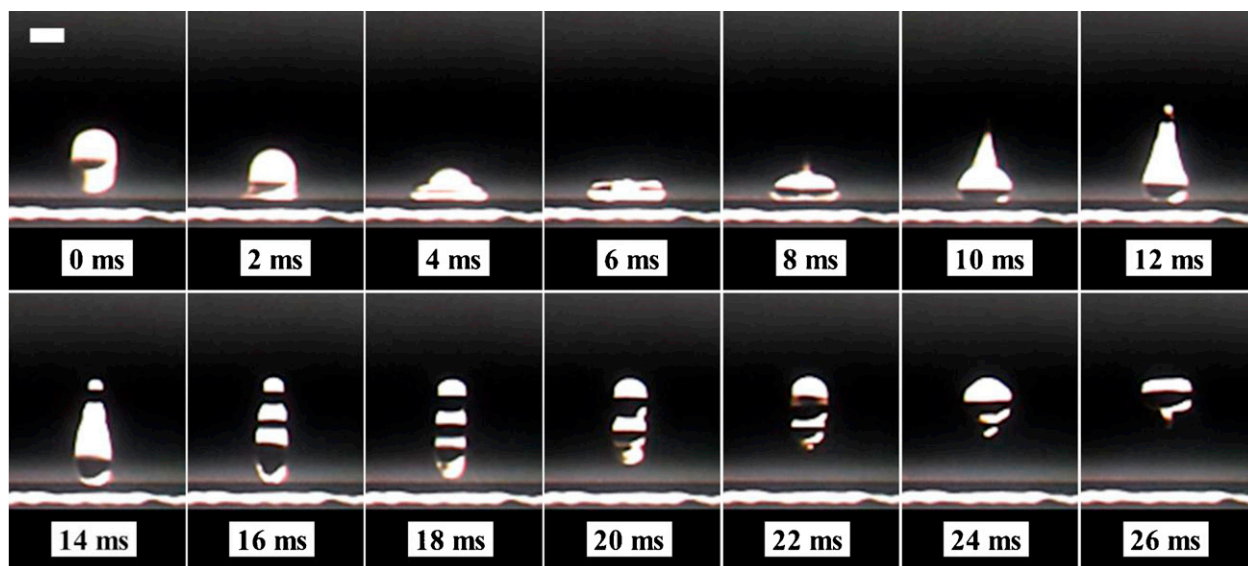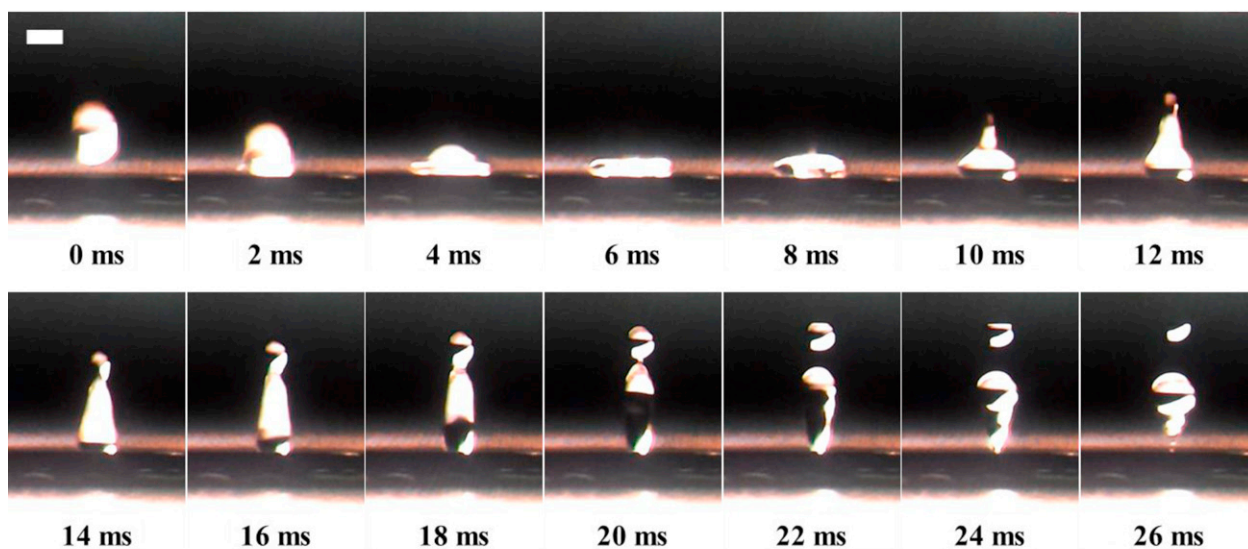

Fig. 5. Captured CCD images of the water droplets placed on each surface after the FC coating. (a) Flat surface (θ_f = 111.6 ± 1.6°), (b) single-scale micro-roughened surface (θ_m = 137.9 ± 1.3°), (c) single-scale nano-roughened surface (θ_n = 150.2 ± 1.4°), and (d) micro/nano dual-scaled surface (θ_{mn} = 159.4 ± 0.5°).

Fig. 7. Sequential images of a water droplet impinging on the surfaces. (a) On the dual-scaled surface, and (b) on the mono-scale micro-roughened surface (the time interval of the sequential images is 2 ms, and the scale bars represent 2 mm).

protuberances as shown in Fig. 2(e) and (f). Fig. 3 shows the AFM images measured on each surface model. In this case, the scanned surface areas were 5 μm × 5 μm for the flat and nano-roughened surfaces, and 10 μm × 10 μm for the micro-roughened and dual-scaled surfaces. From the AFM analysis, the average roughness (R_a) of the micro- and nano-roughened surfaces was estimated to ~158 and ~64 nm, respectively. This suggests that the surface roughness of the two types of surfaces could be increased considerably compared to ~4.7 nm of the flat surface by roughening the surface using the above-mentioned approaches. In addition, Fig. 3(d) obviously shows that two scales of surface roughness are formed efficiently with geometrical hierarchies through combinations of the sandblasting and AAO processes.

3.2. Surface wetting properties

Fig. 4 shows the measured SCAs for each surface. As shown in Fig. 4, the SCA measured on the micro-roughened surface was 137.9 ± 1.3°, which is ~19% larger than that of the flat surface. This suggests that the surface wettability can be improved easily and efficiently by forming micro-roughness on a solid surface through a simple and inexpensive sandblasting technique. In addition, the wetting properties of the sandblasted micro-roughened surfaces could be enhanced further by forming nano-roughness on them through a nonlithographic AAO process. The highest SCA, which was observed on the dual-roughened surface, was 159.4 ± 0.5°, which indicates ~13 and ~6% improvement compared to those of the sandblasted micro-roughened and nano-protuberance-arrayed surfaces, respectively. The CCD images of the water droplet shapes positioned on each surface with different geometries are shown in Fig. 5. The advancing/receding CAs and CAHs obtained on each surface were plotted in Fig. 6. In case of a micro-roughened surface, the measured CAH was quite large, which means that the wetting property of the surface is still governed by non-slippery Wenzel wetting mode, even though the SCA was ~19% higher
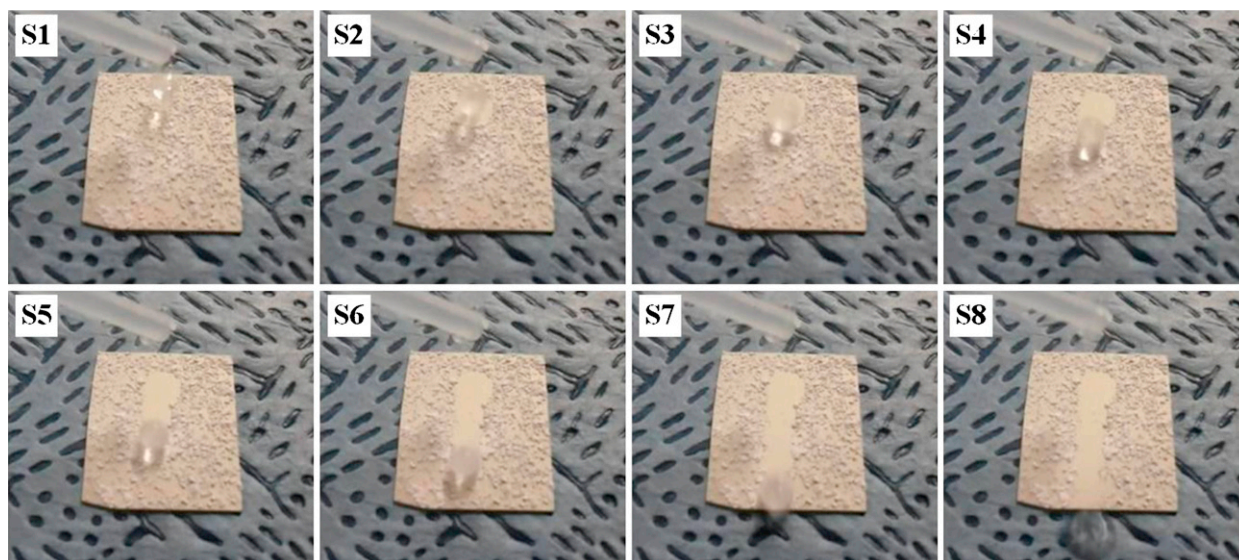
Fig. 8. Captured snap images of a DI water droplet rolling off the fabricated dual-scaled surface covered randomly with silica powders (the tilting angle of the surface is approximately <10° and the time interval of the snap images is 1/30 s).

than that of the flat surface. This implies that the sandblasted micro-structures could be wetted easily by the water droplet due to the gentle slopes of the structures, as shown in Figs. 2(a), (b) and 3(b), resulting in a sufficient increase in roughness factor. The lowest CAH of $3.9 \pm 0.7°$ was obtained on the dual-scaled surface, as shown in Fig. 6. Although the nano-roughened surface also showed a superhydrophobic performance with a considerably low CAH of $9.7 \pm 1.3°$, the superhydrophobicity of the surface could be improved greatly by minimizing the actual contact area between the water droplet and surface, as shown in Fig. 5(d), through the proposed hierarchical approach. This suggests that air pockets, which can support the water droplet, are formed sufficiently between the nano-scale protuberances, resulting in extremely low CAH. In particular, the remarkably low hysteresis of the water contact behavior on the dual-scaled surface enables the proposed surface to sufficiently satisfy the slippery Cassie wetting condition, which is desirable for obtaining attractive self-cleaning and water-repellent properties. These results clearly show that the dual-scaled artificial lotus leaf, ensuring the superhydrophobicity with a CA higher than 159° and a CAH as low as 4°, can be realized efficiently using the proposed simple nonlithographic fabrication approaches.

3.3. Dropping test

Superior water-repellency of such superhydrophobic surfaces is one of the most desirable properties in their practical applications, which require especially nonwetting property of impinging droplet rather than static droplet on a surface [23]. Sequential snapshots, with a time interval of 2 ms, of the water droplet imping-ing the dual-scaled surface are shown in Fig. 7(a). The droplet was deformed maximally spreading along the contact line in 6 ms after impacting and bounced off the surface completely in 18 ms without leaving any satellite drop on the impinged region, which means the contact time of the droplet on the surface is shorter than 18 ms, as shown in Fig. 7(a). The water droplet came to rest on the surface maintaining a high SCA after experiencing several times rebounces. The drop impingement test was also performed on the mono-scale micro-roughened surface with the same initial drop height of ~20 mm and the sequential images were shown in Fig. 7(b). The bouncing behavior of the water droplet on the micro-roughened surface was quite different, although the droplet was

spread with very similar manner after impinging compared to that of the dual-scaled surface. As shown in Fig. 7(b), the water droplet on the micro-roughened surface was stayed ~1.44 times longer than on the dual-scaled surface before bouncing and got stick to the surface after only one-time bounce. In addition, some portion of the droplet was anchored on the surface, and the splitted and tail-like satellites were observed after bouncing in the case of the micro-roughened surface. These phenomena would be originated from the increase in adhesion of the water droplet to the surface due to the significant increment of the contacting area between the water droplet and the surface. These also mean that the anti-wetting pressure cannot exceed the impact pressure and would be because the micro-roughened surface is much sticky due to its high CAH. This experimental observation clearly suggests that the dense array of the fluorocarbon-coated nano-scale pillar-like pro-tuberances on the micro-roughened surface makes it possible to increase sufficiently the antiwetting capillary pressure over the wetting pressure, resulting in a complete nonwetting behavior on the dual-roughened surface. This also provides a concrete evidence for the fact that the proposed dual-scaled surface ensures the super-hydrophobicity in the Cassie wetting mode with a negligible CAH. It was also observed experimentally that the proposed dual-scaled surface can ensure the water-repellency with the increased impact velocity of the water droplet by repeating the dropping tests on the dual-scaled surface as increasing the initial drop height (~50 and ~100 mm). The falling droplets impinging the surface at the increased initial heights were also bounced off completely the sur-face after impinging without remaining satellite droplets on the surface. In addition, the contact time did not changed at each initial drop height although the maximum spreading deformation along the horizontal axis becomes larger as increasing the initial drop height as expected easily [6,23,24].

3.4. Practical self-cleaning test

Fig. 8 shows the snap images of the water droplet, which is rolled off the surface contaminated with silica powders, captured with a time interval of 1/30 s. As shown in Fig. 8, the water droplet was rolled off easily the surface in a short time maintaining its near-spherical shape and the silica powder-covered surface was cleaned completely along the rolling direction of the dispensed

water droplet. This suggests that the dispensed water droplet can collect the dust powders easily and perfectly during rolling off the surface due to the superior superhydrophobic property of the proposed surface. This experimental demonstration clearly supports that the slippery superhydrophobic surface with the prominent self-cleaning ability can be realized efficiently by the proposed simple nonlithographic approach.

4. Conclusion

The micro/nano dual-scaled superhydrophobic surface was demonstrated successfully using a fully nonlithographic simple process that is based on the sandblasting and subsequent AAO techniques with cost-effectiveness. Through the SEM and AFM observations, it was confirmed experimentally that dual-scale hierarchical roughness was well defined on the silicon substrate. The wetting properties of the fabricated surfaces were evaluated by measuring the SCAs and CAHs after a hydrophobic surface coating. The best surface wetting property was observed on the micro/nano dual-roughened surface with the highest SCA of $159.4 \pm 0.5°$ and the lowest CAH of $3.9 \pm 0.7°$ among the surfaces with four different types of surface geometries. The dropping test results revealed clearly that the fabricated dual-roughened surface shows the superior water-repellent behavior with various values of the impact velocity. In addition, it was verified obviously that the proposed dual-scaled surface, which is contaminated with dust particles, can be cleaned easily and perfectly through the practical self-cleaning test. These results clearly show that the proposed fabrication approach can be used simply and efficiently to produce an artificial lotus leaf with prominent superhydrophobicity for further potential applications.

Acknowledgements

References

[1] L. Gao, T.J. McCarthy, The lotus effect explained: two reasons why two length scales of topography are important, Langmuir 22 (2006) 2966–2967.
[2] N.J. Shirtcliffe, G. McHale, M.I. Newton, G. Chabrol, C.C. Perry, Dual-scale roughness produces unusually water-repellent surfaces, Advanced Materials 16 (21) (2004) 1929–1932.
[3] Y.T. Cheng, D.E. Rodak, C.A. Wong, C.A. Hayden, Effects of micro- and nanostructures on the self-cleaning behaviour of lotus leaves, Nanotechnology 17 (2006) 1359–1362.
[4] S.M. Lee, I.D. Jung, J.S. Ko, The effect of the surface wettability of nanoprotrusions formed on network-type microstructures, Journal of Micromechanics and Microengineering 18 (2008) 125007.
[5] Y. Kwon, N. Patankar, J. Choi, J. Lee, Design of surface hierarchy for extreme hydrophobicity, Langmuir 25 (11) (2009) 6129–6136.
[6] L. Chen, Z. Xiao, P.C.H. Chan, Y.-K. Lee, Static and dynamic characterization of robust superhydrophobic surfaces built from nano-flowers on silicon micro-post arrays, Journal of Micromechanics and Microengineering 20 (2010) 105001.
[7] Y. Xiu, L. Zhu, D.W. Hess, C.P. Wong, Hierarchical silicon etched structures for controlled hydrophobicity/superhydrophobicity, Nano Letters 7 (11) (2007) 3388–3393.
[8] Y.-B. Park, M. Im, H. Im, Y.-K. Choi, Superhydrophobic cylindrical nanoshell array, Langmuir 26 (11) (2010) 7661–7664.
[9] Y. Lee, S.-H. Park, K.-B. Kim, J.-K. Lee, Fabrication of hierarchical structures on a polymer surface to mimic natural superhydrophobic surfaces, Advanced Materials 19 (2007) 2330–2335.
[10] H.E. Jeong, S.H. Lee, J.K. Kim, K.Y. Suh, Nanoengineered multiscale hierarchical structures with tailored wetting properties, Langmuir 22 (2006) 1640–1645.
[11] B. Cortese, S. D'Amone, M. Manca, I. Viola, R. Cingolani, G. Gigli, Superhydrophobicity due to the hierarchical scale roughness of PDMS surfaces, Langmuir 24 (2008) 2712–2718.
[12] D.S. Kim, B.-K. Lee, J. Yeo, M.J. Choi, W. Yang, T.H. Kwon, Fabrication of PDMS micro/nano hybrid surface for increasing hydrophobicity, Microelectronic Engineering 86 (2009) 1375–1378.
[13] T.-Y. Kim, B. Ingmar, K. Bewilogua, K.H. Oh, K.-R. Lee, Wetting behaviours of a-C:H:Si:O film coated nano-scale dual rough surface, Chemical Physics Letters 436 (2007) 199–203.
[14] M.-F. Wang, N. Raghunathan, B. Ziaie, A nonlithographic top-down electrochemical approach for creating hierarchical (micro-nano) superhydrophobic silicon surfaces, Langmuir 23 (2007) 2300–2303.
[15] C. Dong, Y. Gu, M. Zhong, L. Li, K. Sezer, M. Ma, W. Liu, Fabrication of superhydrophobic Cu surfaces with tunable regular micro and random nano-scale structures by hybrid laser texture and chemical etching, Journal of Materials Processing Technology 211 (2011) 1234–1240.
[16] Y. Xiu, L. Zhu, D.W. Hess, C.P. Wong, Biomimetic creation of hierarchical surface structures by combining colloidal self-assembly and Au sputter deposition, Langmuir 22 (2006) 9676–9681.
[17] T.O. Yoon, H.J. Shin, S.C. Jeoung, Y.-I. Park, Formation of superhydrophobic poly(dimethylsiloxane) by ultrafast laser-induced surface modification, Optics Express 16 (17) (2008) 12715–12725.
[18] X. Fu, X. He, Fabrication of super-hydrophobic surfaces on aluminum alloy substrates, Applied Surface Science 225 (2008) 1776–1781.
[19] L. Zhang, D.E. Resasco, Single-walled carbon nanotube pillars: a superhydrophobic surface, Langmuir 25 (8) (2009) 4792–4798.
[20] D. Kim, J. Kim, H.C. Park, K.-H. Lee, W. Hwang, A superhydrophobic dual-scale engineered lotus leaf, Journal of Micromechanics and Microengineering 18 (2008) 015019.
[21] Y. Zhang, X. Yu, Q. Zhou, F. Chen, K. Li, Fabrication of superhydrophobic copper surface with ultra-low water roll angle, Applied Surface Science 256 (2010) 1883–1887.
[22] Y. Ohkubo, I. Tsuji, S. Onishi, K. Ogawa, Preparation and characterization of super-hydrophobic and oleophobic surface, Journal of Materials Science 45 (2010) 4963–4969.
[23] Z. Wang, C. Lopez, A. Hirsa, N. Koratkar, Impact dynamics and rebound of water droplets on superhydrophobic carbon nanotubes arrays, Applied Physics Letters 91 (2007) 023105.
[24] D. Richard, C. Clanet, D. Quéré, Contact time of a bouncing drop, Nature 417 (2002) 811.